Shock and Vibration 19 (2012) 1125–1133
DOI 10.3233/SAV-2012-0717
IOS Press

Measurement of join patch properties and their integration into finite-element calculations of assembled structures

A. Schmidt*, S. Bograd and L. Gaul
Institut für Angewandte und Experimentelle Mechanik, Universität Stuttgart, Stuttgart, Germany

Abstract. The vibration and damping characteristics of an assembled structure made of steel are investigated by an experimental modal analysis and compared with the results of a finite element modal analysis. A generic experiment is carried out to evaluate the stiffness and the damping properties of the structure's join patches. Using these results, an appropriate finite element model of the structure is developed where the join patches are represented by thin-layer elements containing material properties which are derived from the generic experiment's results. The joint's stiffness is modeled by orthotropic material behavior whereas the damping properties are represented by the model of constant hysteresis, leading to a complex-valued stiffness matrix. A comparison between the experimental and the numerical modal analysis shows good agreement. A more detailed damping model in conjunction with an optimization procedure for the joint's parameters results in an improved correlation between the experimental and the numerical modal quantities and reveals that the results of the generic experiment are sound.

Keywords: Damping, constant hysteresis, finite element method, thin-layer elements

1. Introduction

Vibrating mechanical systems assembled from metallic components dissipate energy due to the existence of damping. Besides the loss of energy in the material itself (material damping) especially the join patches contribute to the energy dissipation since microslip within the contact surfaces cannot be avoided. As long as the excitation forces do not exceed a certain level, the damping properties are nearly linear with respect to the excitation level. In addidtion, experimental investigations show that the stiffness and the damping properties of materials as well as those of the joints are nearly frequency independent [1].

For numerical simulations of the dynamical behavior of structures, the finite element method (FEM) has established itself as a standard tool. Even though the mass and the stiffness distribution of a structure can be modeled within the FEM quite precisely, there is still a lack of suitable damping models. Classical approaches such as the Rayleigh damping or the identification of relaxation or creep functions by a Prony series result in a high frequency dependency of the damping properties which is in contrast to the results from respective measurements [2,3]. Other approaches such as the use of fractional derivatives [4,5] are not available within commercial software programs. Another option offered by some FE codes is the 'constant hysteretic model' often introduced as 'structural damping'. This model assumes frequency independent damping properties, i.e. the hysteresis in a stress-strain diagram encloses the same area for all frequencies (and constant amplitude) [6,7]. Since the model leads to non-causal behavior in time-domain calculations [8] it can only be used in the frequency domain where one obtains a complex stiffness matrix.

*Corresponding author: A. Schmidt, Institut für Angewandte und Experimentelle Mechanik, Universität Stuttgart, Pfaffenwaldring 9, 70550 Stuttgart, Germany. E-mail: schmidt@iam.uni-stuttgart.de.

ISSN 1070-9622/12/$27.50

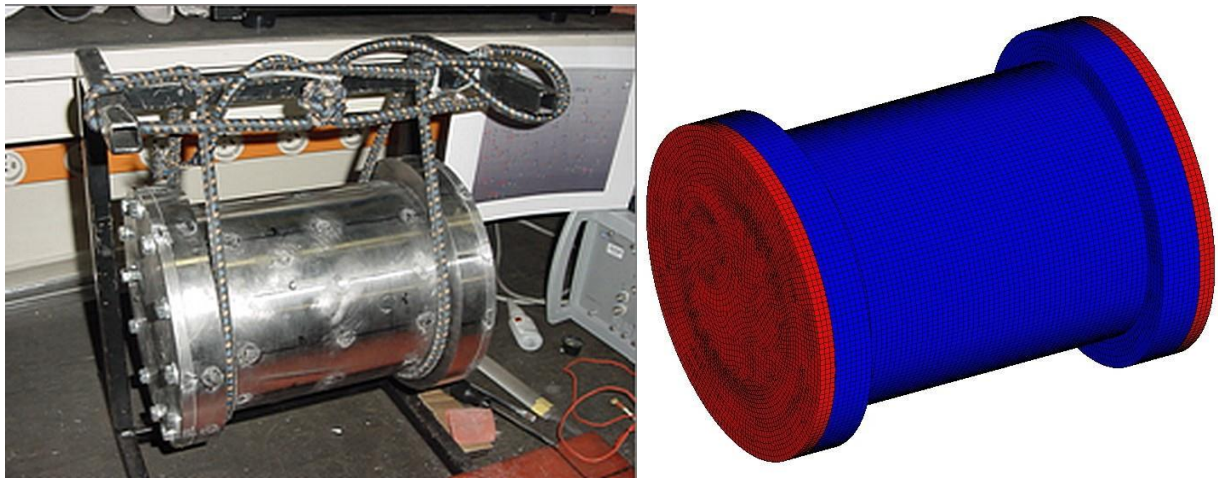

Fig. 1. Investigated structure (left) and its Finite-Element model (right).

Depending on the location of a join patch within a structure, its contribution to the energy dissipation changes from mode to mode. This is why – in contrast to material damping – the damping properties of joints have to be modeled locally. In this case, a modal analysis of the structure leads not only to complex eigenvalues but also to complex eigenvectors which have to be identified by a complex eigenvalue solver.

2. Structure and its FE model

The structure under consideration consists of a hollow cylindrical body (wall thickness: 8 mm) with flanges on its ends, which is enclosed by two circular cover plates (10 mm thick), each mounted with 12 bolts (M8, see Fig. 1, left). The join patches are located between the body and its cover plates. In order to detect the tangential stiffness and loss factor of the joints, a so-called generic joint experiment is performed (see Fig. 2). The set-up consists of two masses m_1 and m_2 connected by a lap joint, which has the same surface finish as the joints of the structure. The normal pressure is nearly constant within the area of contact due to a sufficient thickness of the lap. Its magnitude can be adjusted by a bolt and is calculated from the signal (normal force F_n) of a piezoelectric washer. The normal force is adjusted to obtain the same contact pressure as in the assembly. Mass 2 is excited by an electro-mechanic shaker with a sine input signal. Once the vibration reaches a constant level, the accelerations a_1 and a_2 on both sides of the joint are acquired. These signals are integrated twice with respect to time to receive the absolute displacement. By taking the difference between them, the relative displacement in the joint is determined. The tangential force transmitted by the joint is calculated as a product of the mass m_1 and its acceleration a_1. Knowing the transmitted force and relative displacement, a force-displacement diagram is constructed (see Fig. 3) where the loss factor

$$\eta = \frac{W_D}{2\pi U_{\max}} \tag{1}$$

is calculated from the area W_D enclosed by the hysteresis curve (representing the dissipated energy) devided by the 2π-fold of the maximal stored energy $U_{\max}$ [9]. The slope of the hysteresis loop specifies the tangential stiffness k of the joint.

The FE calculations are run with MSC.Nastran. In the respective model (Fig. 1, right), the join patch is represented by so-called thin-layer elements (TLEs). These elements are ordinary brick elements (Hexa8 with full integration, which are also used for the discretization of the whole structure) whose thickness is considerably smaller that their length or width. Investigations have shown that ratios in the range from 1:100 to 1:1000 do not cause any numerical problems [10]. In order to convert the measured stiffness k from the generic joint experiment to material

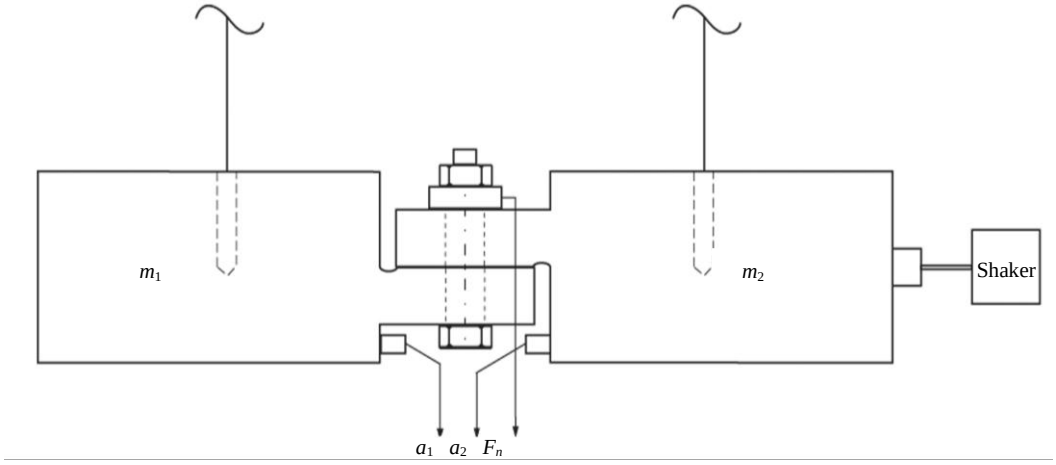

Fig. 2. Set-up of the generic experiment.

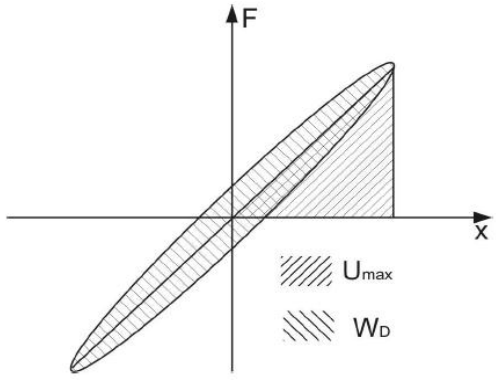

Fig. 3. Hysteresis curve.

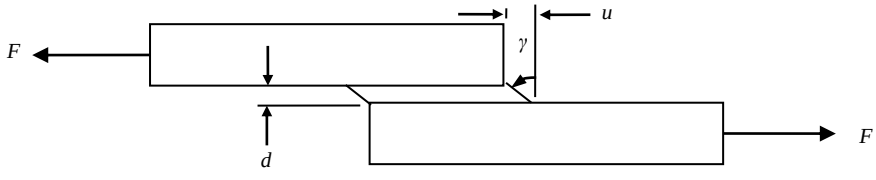

Fig. 4. Schematic joint.

parameters of the TLEs, a schematic of an respective joint is depicted in Fig. 4. The force F acting on both sides of the joint produces a shear stress τ in the TLE. This stress can be expressed as

$$\tau = G\gamma \approx G\frac{u}{d} \tag{2}$$

where G is the shear modulus, γ is the shear strain, u is the displacement and d is the thickness of the TLE. The shear stress can also be expressed as the ratio of the applied tangential force F and the area of the contact A

$$\tau = \frac{F}{A}\ . \tag{3}$$

By combining Eqs (2) and (3) the force can be calculated

$$F \approx \frac{GA}{d} u = ku . \tag{4}$$

From Eq. (4) one finally obtains

$$G = \frac{kd}{A} . \tag{5}$$

Since the join patch shows different stiffness and damping properties in normal and in tangential direction, an orthotropic material model has to be used for the TLEs. The respective material matrix reads

$$\begin{bmatrix} \sigma_{xx} \\ \sigma_{yy} \\ \sigma_{zz} \\ \sigma_{xy} \\ \sigma_{yz} \\ \sigma_{zx} \end{bmatrix} = \begin{bmatrix} E_{11} & E_{12} & E_{13} & 0 & 0 & 0 \\ E_{12} & E_{22} & E_{23} & 0 & 0 & 0 \\ E_{13} & E_{23} & E_{33} & 0 & 0 & 0 \\ 0 & 0 & 0 & E_{44} & 0 & 0 \\ 0 & 0 & 0 & 0 & E_{55} & 0 \\ 0 & 0 & 0 & 0 & 0 & E_{66} \end{bmatrix} \begin{bmatrix} \varepsilon_{xx} \\ \varepsilon_{yy} \\ \varepsilon_{zz} \\ \varepsilon_{xy} \\ \varepsilon_{yz} \\ \varepsilon_{zx} \end{bmatrix} \tag{6}$$

where z denotes the normal direction of the joint's interface. For the TLEs all off-diagonal terms in Eq. (6) vanish since no transversal contraction occurs within the contact surface. In addition, as the interface obeyes no stiffness in x- and y-direction, the terms E_{11} and E_{22} are zero. Since the joint also exhibits no stiffness for in-plane shearing, E_{44} vanishes as well. E_{33} represents the normal stiffness, whereas $E_{55} = E_{66}$ define the tangential stiffness of the joint. The relations between E_{55} and E_{66} with the shear moduli G_{zx} and G_{zy} are

$$E_{55} = 2G_{zy} \quad \text{and} \quad E_{66} = 2G_{zx} . \tag{7}$$

For numerical reasons the values of E_{11}, E_{22}, and E_{44} entered in the FEM software must be different from zero but are set to a value some magnitudes smaller than those for E_{33}, E_{55}, and E_{66}. Once the stiffness matrix $\boldsymbol{K}$ and the mass matrix $\boldsymbol{M}$ are calculated from the FE software, the eigenvalue problem of the undamped system with n degrees of freedom can be solved from

$$\left(\boldsymbol{M} \lambda_i^2 + \boldsymbol{K} \right) \boldsymbol{\varphi}_i = 0 , \tag{8}$$

where λ_i are the n (real) eigenvalues and $\boldsymbol{\varphi}_i$ the respective (real) eigenvectors. Using the model of constant hysteresis, the equation is extended to [1]

$$\left(\boldsymbol{M} \lambda_i^{*2} + \mathrm{i}\, \boldsymbol{D} + \boldsymbol{K} \right) \boldsymbol{\varphi}_i^* = \left(\boldsymbol{M} \lambda_i^{*2} + \boldsymbol{K}^* \right) \boldsymbol{\varphi}_i^* = 0 , \tag{9}$$

where the superscript $\bullet^*$ shall denote complex quantities. The damping matrix $\boldsymbol{D}$ is constructed from the TLEs as the real stiffness matrix $\boldsymbol{K}_{TLE}$ derived from Eq. (6) multiplied by the loss factor η from the generic experiment, see Eq. (1). Thus, the complex stiffness matrix $\boldsymbol{K}_{TLE}^*$ of a TLE reads

$$\boldsymbol{K}_{TLE}^* = \boldsymbol{K}_{TLE} \left(1 + \mathrm{i}\, \eta_{TLE} \right). \tag{10}$$

The system matrices are then assembled from all element matrices. Note that within this formulation the loss factor in normal and in tangential direction are identical.

3. Experimental results

The EMA of the assembled structure is performed up to 4.5 kHz using a tri-axial piezo accelerometer and 90 excitation points. In this way, 14 modes are identified through the given frequency range. The eigenfrequencies and the respective modal damping values are given in Table 1. Due to the symmetry of the structure double modes appear except for modes 5 and 6 (see Fig. 6). All other modes are either tubular modes (1 to 4 and 11 to 14), bending modes (7 and 8), or shear modes (9 and 10); torsional modes cannot be detected by this set-up.

The generic joint experiment is performed in a frequency range from 200 Hz up to 1500 Hz in order to stay well below the first eigenfrequency of the set-up. Since the identified stiffnesses and loss factors do not change notably with the frequency, the assumption of a constant hysteresis is confirmed [3]. The identified values are

$$k = 520 \frac{\text{kN}}{\text{mm}} \quad \text{and} \quad \eta = 0.028, \tag{11}$$

where especially the loss factor shows some uncertainty which can be seen if a measurement is repeated with the same contact pressure and excitation after the set-up of the generic experiment is unmounted and re-assembled.

Table 1
Eigenfrequencies and modal damping values: EMA and FEM

	Eigenfrequency [Hz]			Modal damping [%]		
Mode #	EMA	FEM	Diff [%]	EMA	FEM	Diff [%]
1	2038	2016.8	−1.04	0.06979	0.09082	30.14
2	2084	2017.3	−3.20	0.06979	0.09077	30.06
3	2809	2904.5	3.40	0.07633	0.05046	−33.89
4	2874	2918.5	1.55	0.07633	0.05024	−33.19
5	2961	2999.6	1.30	0.3135	0.08832	−71.83
6	3277	3301.9	0.76	0.3012	0.1001	−66.75
7	3986	3913.7	−1.81	0.1369	0.1003	−26.77
8	3988	3914.1	−1.85	0.1369	0.1002	−26.82
9	4242	4224.8	−0.41	0.1130	0.04601	−59.28
10	4251	4225.1	−0.61	0.1130	0.04604	−59.26
11	4353	4092.9	−5.98	0.1369	0.1575	15.08
12	4353	4093.3	−5.97	0.1369	0.1575	15.06
13	4462	4601.5	3.13	0.03198	0.03222	0.75
14	4462	4629.0	3.74	0.03198	0.03217	0.59

4. FE results and optimization

The structure is discretized with nearly 70000 brick elements (8-noded; linear shape functions) resulting in more than 263000 dof. Neither the bolts nor the holes are included in the FE model. For both join patches a single layer, each consisting of 1391 TLEs is used whose thickness is chosen as d = 0.1 mm (see Fig. 5). Since the contact area A = 1087 mm^2 of the generic experiment is known, the entries of the material matrix can be calculated from Eq. (5) and Eq. (7) as

$$E_{55} = E_{66} = 95.7 \frac{\text{N}}{\text{mm}^2}. \tag{12}$$

No measurements are available for the joint's normal stiffness. Since it must be smaller than the material's normal stiffness but essentially larger than the tangential joint's stiffness, as a first guess, E_{33} is estimated to 5000 N/mm^2. The material data for the structure itself (steel, isotropic) is taken to be E = 207500 N/mm^2 for the

cylinder and $E = 210000\ \mathrm{N/mm^2}$ for the cover plates, the density is $\rho = 7790\ \mathrm{kg/m^3}$, and Poisson's ratio $\nu = 0.3$. A FE modal analysis is carried out using upper Hessenberg method.

A comparison between the measured and the calculated eigenfrequencies of the first 14 modes shows a mean absolute deviation of only 1.8%. Except for modes 5 and 6, also the calculated modal damping values are in good agreement with the measured results (see Table 1) keeping in mind the uncertainty in detecting the loss factor from the generic experiment and the simple representation of damping in the FE model. A closer look at modes 5 and 6 (Fig. 6) reveals that the bolts and their threads are heavily involved in the referring modal deformations. Since the bolts, their threads and the bore holes are neglected in the FE model, the corresponding damping effects are not accounted for in the numerical calculation. This is why the calculated damping of these modes is notably underestimated.

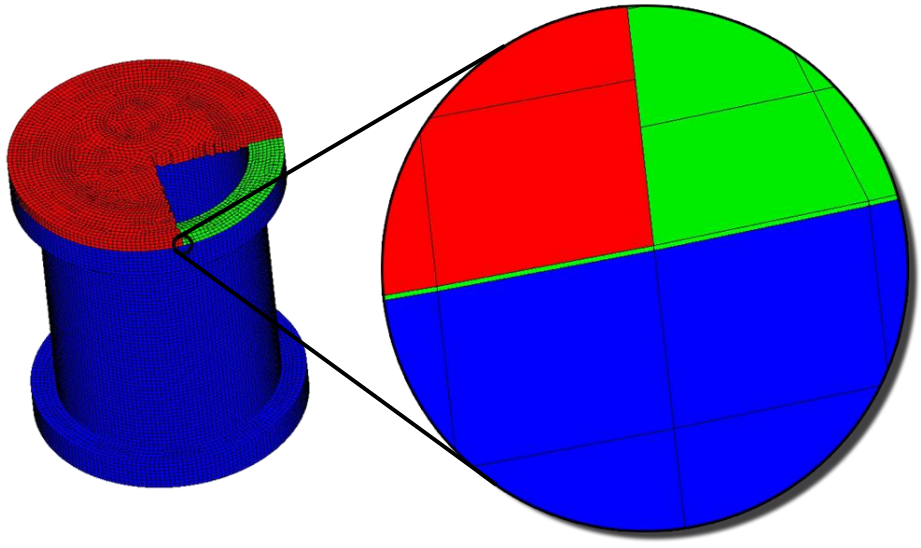

Fig. 5. FE model of the structure and its join patch.

In order to incorporate the damping effects of the bolts, a second loss factor η^n_{TLE} for the damping in normal direction of the TLEs is introduced. Thus, the respective dissipation is not modeled at the exact location of the bolts but is considered as an 'integrative effect' of the join patch. Accordingly, the stiffness matrix of each TLE is split into a tangential part (index t) and a normal part (index n)

$$\boldsymbol{K}_{TLE} = \boldsymbol{K}^t_{TLE} + \boldsymbol{K}^n_{TLE}, \tag{13}$$

resulting from the material matrix Eq. (6) which is also split into tangential part with the entries E_{55} and E_{66} and a normal part, containing only the entry E_{33}. The complex stiffness matrix $\boldsymbol{K}^*_{TLE}$ of each TLE is then given by

$$\boldsymbol{K}^*_{TLE} = \boldsymbol{K}^t_{TLE}\left(1 + i\eta^t_{TLE}\right) + \boldsymbol{K}^n_{TLE}\left(1 + i\eta^n_{TLE}\right). \tag{14}$$

Since neither the stiffness nor the damping properties of the joint in normal direction are available, a parameter identification is executed. To this end, an optimization procedure is coded in Matlab, where the loss factors η^t_{TLE} and η^n_{TLE} as well as the moduli E_{33} and $E_{55} = E_{66}$ of the TLEs are taken as free variables. The procedure is run with the 'lsqnonlin' command which minimizes the residuum r from the measured and the calculated data (eigenfrequencies f_i and percentage modal damping η_m) in a least-squares sense for non-linear problems

$$\min r = \min \sum_i \left(f_i^{exp} - f_i^{FEM} \right)^2 + \left[w\left(\eta_{m,i}^{exp} - \eta_{m,i}^{FEM} \right) \right]^2. \tag{15}$$

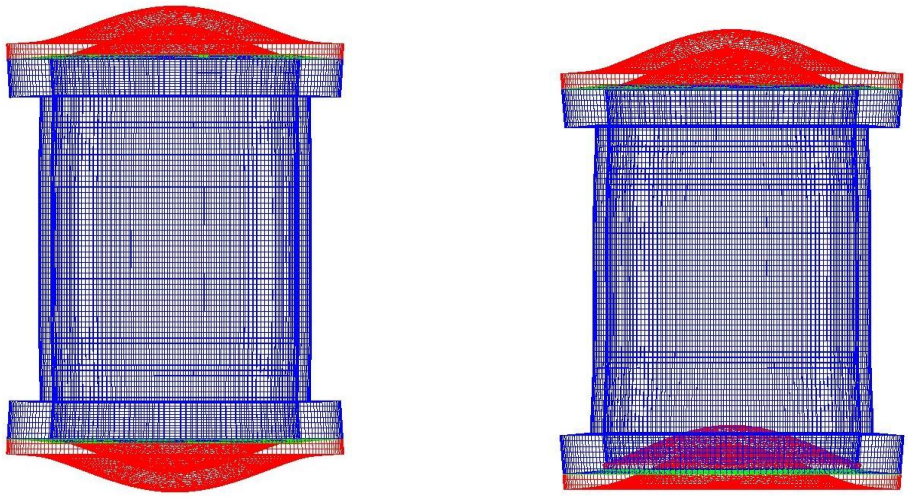

Fig. 6. Visualization of mode 5 and mode 6.

As the modal damping values are by some orders of magnitude smaller than the eigenfrequencies, a weighting factor $w = 5 \cdot 10^5$ is introduced in Eq. (15). Initially, the portion of the residuum caused by the modal damping values is approximately 10 times greater than the one caused by the eigenfrequencies and will roughly be of the same size by the end of the parameter identification. During the optimization, Matlab runs Nastran with different sets of parameters to test the sensitivity of the residuum r on the free parameters and then reduce it step by step. The whole procedure takes some hours as each numerical modal analysis in Nastran lasts about 10 minutes. Special care has to be taken due to the swapping of modes in the numerical calculation for different sets of parameters and the absence of torsional modes in the EMA. Thus, the mode shapes are identified after each Nastran run and the eigenfrequencies and the modal damping values are related to the equivalent measured ones in Eq. (15).

The optimization results (TLE parameters) are given in Table 2 together with their starting values. Since the tangential stiffness of the join patch gained from the generic experiment is reliable, the change of E_{55} and E_{66} during the optimization are limited to approximately $\pm 25\%$. For the free parameters in normal direction whose starting values were estimated, substantial changes are obtained by the optimization. The loss factor in tangential direction which was found by the generic experiment changes only moderately.

Table 2
Identified parameters of the TLEs

	E_{55}, E_{66} [N/mm^2]	E_{33} [N/mm^2]	η^t_{TLE} [−]	η^n_{TLE} [−]
Start value	96.4	5000.0	0.028	0.028
Optimized value	120.0	914.2	0.0235	0.0818
Difference [%]	+24.5	−81.7	−16.1	+192.1

In Table 3 the eigenfrequencies and modal damping values at the end of the optimization are given together with the respective measured quantities. Compared to the starting values of the free parameters, the resiuduum r is reduced by 86.4%. The average deviation of the eigenfrequencies is 2.57% whereas the difference of the modal damping values is reduced substantially to 19.59%, which can be seen as an excellent correlation.

5. Conclusions

The use of thin-layer elements in conjunction with the model of constant hysteresis is an appropriate approach to model the damping properties of assembled structures in finite element calculations. It allows to model the damping

Table 3
Eigenfrequencies and modal damping values after optimization: EMA and FEM

	Eigenfrequency [Hz]			Modal damping [%]		
Mode #	EMA	FEM	Diff [%]	EMA	FEM	Diff [%]
1	2038	2021.3	−0.82	0.06979	0.09454	35.47
2	2084	2021.8	−2.98	0.06979	0.09449	35.39
3	2809	2923.9	4.09	0.07633	0.04836	−36.64
4	2874	2910.0	1.25	0.07633	0.04858	−36.36
5	2961	2902.0	−1.99	0.3135	0.3244	3.46
6	3277	3209.4	−2.06	0.3012	0.3040	0.91
7	3986	3919.3	−1.67	0.1369	0.1108	−19.09
8	3988	3919.7	−1.71	0.1369	0.1107	−19.12
9	4242	4213.1	−0.68	0.1130	0.07398	−34.53
10	4251	4213.4	−0.88	0.1130	0.07401	−34.51
11	4353	4117.9	−5.40	0.1369	0.1475	7.76
12	4353	4118.3	−5.39	0.1369	0.1475	7.75
13	4462	4604.3	3.19	0.03198	0.03148	−1.57
14	4462	4631.8	3.81	0.03198	0.03143	−1.72

locally and thus results in complex eigenvalues and eigenvectors. In contrast to global damping models, modes with high or low modal damping values can be identified. This fact can be essential, if the crucial (low-damped) eigenfrequencies of a structure shall be identified in the design phase in order to modify the construction before any prototype is produced. While the eigenfrequencies and the eigenmodes can be predicted by the FEM to a high degree of accuracy, the predicted damping values may notably differ from measured values. This is due to many uncertainties in the FE model but also a result of significant scattering of measured damping values. Nevertheless, a qualitative prediction of modes with high damping and lowly-damped modes is possible.

The constant hysteretic damping model obviously fits measured data much better than classical models such as the Rayleigh damping or other approaches with velocity-proportional damping forces. The model needs only one parameter (for a 1d problem) which can easily be identified. However, time-domain calculations are not possible with this damping model since it leads to non-causal behavior.

A so-called generic experiment is introduced which proves to be an appropriate way to measure the stiffness and the energy losses in joints of assembled structures. Nevertheless, a parameter optimization in conjunction with a more detailed model of the damping properties reveals potential for further improvements.

Acknowledgments

The financial support of the DFG (Deutsche Forschungsgemeinschaft) and the FVV (Forschungsvereinigung Verbrennungskraftmaschinen) and the support of AtlasCopco is gratefully acknowledged.

References

[1] L. Gaul, A. Schmidt and S. Bograd, *Joint damping prediction by thin layer elements*, Proceedings of IMAC XXVI: A Conference & Exposition on Structural Dynamics, Orlando, FL, USA, February 4−7, 2008, CD-ROM.
[2] K.J. Bathe and E.L. Wilson, *Numerical Methods in Finite Element Analysis*, Prentice Hall, 1976.
[3] S. Bograd, A. Schmidt and L. Gaul, *Experimentelle Bestimmung von Kennwerten zur Werkstoff- und Fügestellendämpfung sowie deren Berücksichtigung in Finite-Elemente-Berechnungen*, Abschlussbericht, Forschungsvereinigung Verbrennungskraftmaschinen (FVV), Heft 859, Frankfurt, 2008
[4] K.B. Oldham and J. Spanier, *The Fractional Calculus*, Academic Press, 1974.
[5] R.S. Lakes, *Viscoelastic Solids*, CRC Press, 1999.
[6] M. Ganapathi, B.P. Patel, P. Boisse and O. Polit, Flexural loss factor of sandwich and laminated composited beams using linear and nonlinear dynamic analysis, *Composites: Part B* **30** (1999), 245−256.

[7] X. Chen, H.L. Chen and X.L. Hu, Damping prediction of sandwich structures by order-reduction- iteration approach, *Journal of Sound and Vibration* **222**(5) (1999), 803−812.
[8] L. Gaul, S. Bohlen and S. Kempfle, Transient and forced oscillations of systems with constant hysteretic damping, *Mechanics Research Communications* **12**(4) (1985), 187−201.
[9] D. Thorby, *Structural Dynamics and Vibration in Practice*, (1st ed.), Elsevier, 2008.
[10] G. Pande and K. Sharma, On joint/interface elements and associated problems of ill-conditioning, *International Journal for Numerical and Analytical Methods in Geomechanics* **3** (1979), 293–300.